Part I
Microreactor Design, Fabrication and Assembly

1
Silicon and Glass Microreactors

Roald M. Tiggelaar and J. G. E. (Han) Gardeniers

1.1
Introduction

Due to their small characteristic dimensions, microreactors have fundamental advantages in comparison with conventional macro-scale systems. As a consequence, microreactors are suitable for performing and/or studying reactions under relatively safe conditions, which is important in the case of potentially dangerous processes, such as highly exothermic reactions, reactions in which flammable, explosive or toxic chemicals are involved or reactions that require harsh conditions in terms of temperature or pressure. In fact, microreactors open the way to new operating regimes and applications [1, 2].

Although microreactors can be realized in many materials, such as polymers (e.g. PMMA, PDMS, SU-8), stainless steel and ceramics, (for details, see [3]), this chapter will focus on the design, fabrication and assembly of microreactors made of silicon and glass.

Silicon is known for its chemical inertness, purity, good mechanical and electrical properties and excellent thermal properties. For silicon, a large amount of techniques is available to produce small structures, in addition to methods to passivate these geometries with chemically well-known inert and electrically and thermally insulating layers (e.g. SiO_2, Si_3N_4) [4–6]. These silicon micromachining processes are robust and have excellent precision. Due to its origin in the semiconductor industry [7], silicon micromachining offers the opportunity of integration of electronic control functionality (sensors and actuators). High-density integration of e.g. heating filaments and temperature sensors allows local heating and well-controlled steep temperature gradients. This implies that not the whole microreactor has to be at an elevated temperature, as is the case for most stainless-steel and ceramic microreactors, which not only results in an efficient way of heating, but also allows that the temperature required to perform a reaction can be addressed to well-defined locations of the system. As a consequence, reactions that need elevated temperatures for a short period can be controlled easily: local heating of reactants can be performed

Micro Process Engineering, Vol. 2: Devices, Reactions and Applications.
Edited by V. Hessel, A. Renken, J.C. Schouten, and J.-I. Yoshida

ISBN: 978-3-527-31550-5

on a short time-scale (milliseconds) and fast cooling can be achieved in order to quench reactions and prevent runaway.

Vitreous materials such as glass are attractive materials for microreactors due to their compatibility with a wide range of solvents and electrical and thermal insulating properties. Another important feature of glass is its transparency: this facilitates on-line optical monitoring of reactions performed in glass based microreactors, e.g. with a microscope or fluorescence detection, and it also helps in the optimization of fluidic control in microchannel networks, of mixing and of the establishment of the desired flow regime in two-phase flow systems. Many techniques for fabricating microfluidic structures in glass are known, and also for the integration of electronic control functionality [8, 9].

The processes used to fabricate microreactors of silicon and glass include photolithography, wet chemical etching, deep reactive ion etching (DRIE) and growth or deposition of layers of silicon dioxide (SiO_2), silicon nitride (SiN) and metals. With proper mask materials (resist, SiO_2 and/or SiN) in combination with DRIE, fluidic structures that have rectangular cross-sections can be made in silicon. If silicon is processed with wet etchants such as potassium hydroxide (KOH) or tetramethyl-ammonium hydroxide (TMAH), flow channel cross-sections are trapezoidal or rectangular, depending on the crystal orientation of the silicon substrate. Glass is commonly processed with (buffered) hydrofluoric acid [(B)HF] solutions and mask layers of resist, polysilicon or metal, resulting in fluidic channels with nearly half-circular cross-sections. Integration of control functionality, usually thin films of platinum with an adhesion metal (Cr, Ti or Ta), is often done via physical vapor deposition (sputtering or evaporation) in combination with a lift-off process or shadow masking. Assembly of microreactors via enclosure of flow channels with other substrates containing access holes to the channel structure, made by milling, drilling, powder blasting or etching methods, can be done by means of gluing, clamping or wafer bonding. Fundamentals of all the mentioned techniques and methods can be found elsewhere [4, 5, 8].

1.2 Design and Fabrication of Microreactors for Heterogeneous Catalysis

Microreactors offer improved heat and mass transfer rates due to the smaller distances for transport and increased surface-to-volume ratio, leading to more efficient interactions between species in different phases. This is the main reason to use them for rapid, safe, easy, efficient and reliable development and screening of heterogeneous catalysts. Microreactors offer new opportunities to investigate catalytic materials for selectivity, yield and conversion as a function of catalyst in addition to reactant composition, temperature, residence time and pressure. Moreover, in addition to studying the kinetics of catalytic reactions (e.g. rate order, rate constants, activation energies, ignition temperatures, equilibrium temperature coefficients), microreactors are nowadays also used for small-scale and on-demand manufacturing of fine chemicals via (direct) catalytic partial oxidation reactions, portable fuel cell

applications, hydrogen and synthesis gas production and purification and the utilization of natural gas resources.

An important topic of research is the introduction of the catalyst in the microreactor. In brief, solid catalysts can be incorporated on the interior of micromachined reaction channels, prior to or after closure of the channel, by a variety of strategies: anodic oxidation, plasma–chemical oxidation, flame combustion synthesis, sol–gel techniques, impregnation, wash coating, (electro-)plating, aerosols, brushing, chemical vapor deposition, physical vapor deposition and nanoparticle deposition or self-assembly. Some of these methods can be applied in combination with photolithography or shadow masking.

For characterization, in most set-ups the microreactor is mounted on a custom-built block of a metal (stainless steel, aluminum) or ceramic using glue or a screw-clamped sealing cover of metal or acrylic that might have an opening for microscopic inspection of the microreactor during operation. Fluidic connections between this block and mass flow controllers, syringes and analysis equipment are made by valves, stainless-steel tubes with Swagelock fittings, Teflon or PTFE tubing glued with inorganic resins and/or capillaries fixed by ceramic cement. Gas-tight and leak-free feedthrough connections between the microreactor and block with fluidic fixtures are obtained by sealing O-rings and ferrules (Viton, Kalrez, Kapton, gold), elastomeric gaskets, graphite tape or other materials that are slightly compressed during mounting of the microreactor. Equipment and techniques used to analyze and quantify the product and species formed in microreactors are (quadrupole) mass-spectrometry [(Q)MS], ^{1}H nuclear magnetic resonance (^{1}H NMR) spectroscopy, (micro) gas chromatography (GC) and/or Fourier transform infrared (FT-IR) spectrometry. More details about process analysis can be found in Volume 3 of this Handbook.

Computer-controlled heating and temperature control of the microreactor are performed via two concepts. If the microreactor is *not* equipped with integrated heating filaments, the whole microreactor is brought to elevated temperatures via heater cartridges positioned in the block on which the microreactor is mounted or by placing the mounted microreactor in a furnace/oven. In this 'block-heating' concept, the temperature of the reactor is measured and controlled via thermocouples inserted in the block and/or in special wells in the microreactor. If the microreactor, however, contains on-chip integrated thin-film heaters and *in situ* sensors, elevated temperatures can be reached in well-defined locations only, i.e. the reaction zone, thereby providing efficient heating with low amounts of electrical energy. In this 'local-heating' concept, electrical connections between the microreactor and control equipment are made with probe-cards, soldered wires or special constructed printed circuit boards (PCBs) with spring connectors.

1.2.1 Low-temperature Microreactors

Up to the boiling point of liquid reactants, two- and three-phase heterogeneous catalytic reactions are carried out in microreactors using the block-heating concept

described above. For example, in a (100)-silicon/Pyrex reactor with a T-shaped channel with two inlets and one outlet, zeolite-based catalysts were studied in a reaction channel of 33 mm × 200–1000 μm × 220–250 μm. Prior to closure of the channel, different zeolites (silicalite-1, aluminum ZSM-5 and titanium silicate-1, TS-1) were deposited via sequences of grafting, (confined) seeding, (regrowth) synthesis, (selective) deposition, etching and calcinations steps [10–13]. After characterizing the influence of thickness, morphology and crystal orientation on the catalyst activity, 1-pentene epoxidation with hydrogen peroxide over TS-1 catalyst was performed, with an enhanced reactivity (up to 100 °C) [14, 15].

In an another study, in a glass microreactor with a serpentine-shaped channel with three inlets and one outlet (length 45 cm, cross-sectional radius 100 μm), triphase reactions were performed at room temperature [16]. Palladium was immobilized on the glass walls via flushing an amine and a micro-encapsulated Pd solution through the channel and heating and cross-linking. The microreactor was operated in such a manner that the liquid film formed on the channel wall was separated from the gas phase in the center of the channel. To prove this concept, Pd-catalyzed hydrogenation reactions were carried out at room temperature for a variety of substrates [13, 16].

In a packed-bed microreactor (Figure 1.1a), the kinetics were investigated of the ambient temperature gas–liquid–solid hydrogenation of cyclohexene to cyclohexane. In the reaction channel (20 mm × 600–625 μm × 300 μm) etched in silicon, near the two inlets and outlet 25–40 μm wide retainer posts (25 μm spacing) were included, that fix catalyst particles and act as a flow distribution manifold and reactant mixer. The bed consisted of Al_2O_3 beads (35–75 μm) impregnated with Pt that were loaded into the reactor via extra inlet channels by applying a vacuum to the outlet. [17]. Mass transfer rate improvements of up to a factor 100 compared with conventional packed-bed reactors were obtained [18]. This reaction was also studied in microreactors where the active catalyst surface was enhanced up to 250-fold by using parallel channels (Figure 1.1b). In one configuration, an array of 10 parallel packed-bed channels as described above was connected to a reactant supply through a manifold of 500 μm wide channels and the reactants were distributed and mixed by means of small slits at the entrance of each channel. Alternatively, these channels could also be

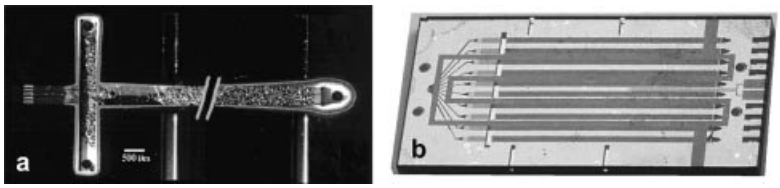

Figure 1.1 Microreactors (40 mm × 15 mm × 1.0–1.5 mm) for gas–liquid–solid Pt-catalyzed cyclohexene hydrogenation at room temperature: (a) single-channel and (b) 10 parallel channel configuration. (a) Reprinted with permission from [18], Copyright 2001 American Chemical Society; (b) reproduced from [19] with permission, Copyright 2002 IEEE.

filled with staggered arrays of pillars (50 μm diameter) with walls of oxidized porous silicon that were impregnated with Pt [19].

1.2.2 High-temperature Microreactors

For higher temperatures (≥100 °C), microreactors are frequently used for investigating catalytic processes in which gases are involved. The silicon packed-bed microreactors shown in Figure 1.1a could withstand corrosive gases when the channel interior was thermally oxidized (5 μm SiO_2) prior to loading of the catalyst. They were applied for small-scale carbon-catalyzed phosgene synthesis up to 250 °C via block-heating [17] and for testing heterogeneous gas-phase catalysts. The latter was also performed in a differential packed-bed cross-flow microreactor with integrated pressure drop channels. This reactor has one inlet and one outlet manifold and these bifurcate into 64 parallel channels (370 μm deep) that feed the catalyst bed (Figure 1.2a). An array of 50 μm wide posts (40 μm spacing) holds the bed of metal-catalyst coated Al_2O_3 particles (53–71 μm) in place and is followed by shallow channels (1.3 mm × 40 μm × 20 μm) to maintain an even flow distribution across the isobaric bed. With this reactor, Rh- and Pt-catalyzed CO oxidations were performed for temperatures up to 175 °C [20, 21] and this reaction was also applied to screen the selectivity of salt-impregnated packed beds of 150 μm γ-Al_2O_3 particles. Beads with catalyst coatings of Co, Cu, Ni, Pd, Rh and Ru were loaded in a microreactor with an array of six parallel channels (1 mm × 0.6–1 mm × 300 μm), fixed with alumina wool [22] and tested up to 250 °C.

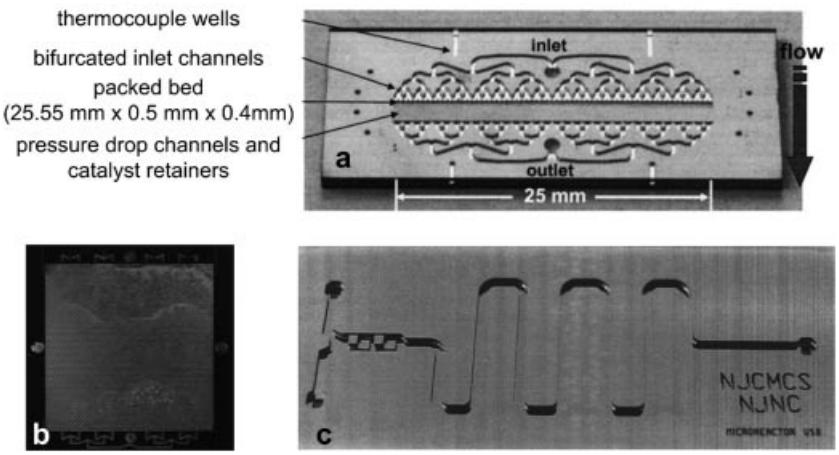

Figure 1.2 Microreactors for (preferential) CO oxidation: (a) differential packed-bed crossflow microreactor (40 × 15 × 1.5 mm) with Rh and Pt catalysts (up to 175 °C); (b) chip (6 × 6 cm) with staggered rows of pillars covered with 10 μm Pt/Al_2O_3 via sol–gel and wash-coating (up to 250 °C); (c) chip with Pt/Al_2O_3 immobilized via sol–gel infiltration (up to 300 °C). Reprinted from [20], Copyright 2002, and [24], Copyright 2004, with permission from Elsevier, and [25].

Metal-catalyzed (preferential) CO oxidation is also often carried out in microreactors with sol–gel-based catalysts, since these catalysts are popular in "conventional" catalysis due to the ease of producing porous structures with tunable pore size and volume, aspects which can also be achieved in microreactors. Uniform thin-film catalysts with well-controlled loads can be synthesized by sol–gel methods using precursors in water-based solvents and surface-selective approaches. For uniform infiltration of the sol–gel catalyst precursor in microfluidic channels, a hydrophobic film can be applied to the top surface of the silicon, while the sidewalls of the channels remain hydrophilic. Under these conditions, the catalyst precursor infiltrates selectively into the channels. Two different approaches were developed: infiltration of the precursor and drying/calcination prior to or after capping of the channels, on which nanosized particles can be dispersed [23]. Using this sol–gel method, a microreactor with a 1.5–3 μm Pt/Al_2O_3 coating in its channel (5.8–54 cm × 100–500 μm × 75–500 μm) was created for preferential CO oxidation studies [23]. This method was also used to form a 10 μm thick Pt layer in the reaction zone (4.5 × 4.5 cm) of a reactor that was filled with staggered rows of silicon pillars (diameter 400 μm, height 200 μm) for efficient mixing (Figure 1.2b) and employed for preferential oxidation of CO in excess H_2 (up to 250 °C using block heating) [24]. More sophisticated sol–gel infiltration techniques made it possible to immobilize Pt/Al_2O_3 catalyst *only* in the reaction channel (45 mm × 500 μm × 600 μm) of a microreactor (Figure 1.2c) and *not* in the inlet zone, mixing channel, quenching channel (via cooling) and outlet zone [25]. Therefore, this microreactor could be used for very detailed studies of catalyzed CO oxidation as a function of catalyst loading and temperatures up to 300 °C.

In microreactors loaded with a Pd/Al_2O_3 layer using a sol–gel technique and impregnation, highly exothermic oxidation reactions were studied (Figure 1.3a). In this catalyst bed (1.5 mm × 10 mm × 200 μm) the full and partial oxidation of methane could be carried out without problems, for stoichiometric and fuel-rich compositions of CH_4–O_2. Resistive heating was accomplished via a piece of silicon (30 mm × 5 mm) placed on the silicon side of the catalyst bed. Ignition and extinction behavior was observed as abrupt temperature fluctuations at 585 and ca. 600 °C and above 615 °C the conversion and activity of Pd decreased due to carbon formation and phase changes [26, 27]. When these microreactors were equipped with an integrated heating element and temperature sensor (Figure 1.3b) that allowed local heating of the catalyst bed, better temperature control of the reaction zone was achieved. Due to reduced thermal response times in this microreactor, no abrupt temperature changes were detected during ignition/extinction for the investigated CH_4–O_2 mixtures (from fuel-lean to fuel-rich) over an Rh/Al_2O_3 catalyst [28]. Other methods to obtain catalytic materials in the catalyst bed of this microreactor are reported, showing the versatility of these devices. Colloid nanoparticles of Pt/Ru could be embedded by flushing and evaporation steps and Cs- or Ba-promoted Ru/C catalysts on porous graphite by flushing with sucrose and pyrolysis. These catalysts were used for the oxidation of CO (up to 340 °C) and ammonia decomposition (up to 230 °C), respectively [29, 30].

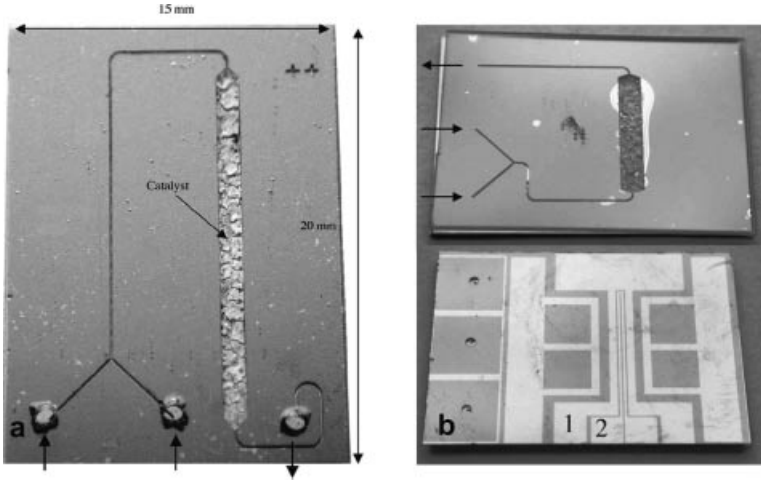

Figure 1.3 (a) Microreactors (20 × 15 mm) with catalysts of Pd, Pt and Rh impregnated on sol–gel-based Al_2O_3 for full and partial oxidation of methane (up to 600 °C), (b) with an on-chip $NiSi_2$ heater and sensor (on back side of reaction zone). Reprinted from [27], Copyright 2005, and [28], Copyright 2006, with permission from Elsevier.

Physical vapor deposition with shadow masks is known for its simplicity for creating defined areas of thin-film catalytic material in microreactors. This technique was used to deposit silver in the reaction manifolds of microreactors for small-scale synthesis of valuable fine chemicals (Figure 1.4a). The manifolds consisted of a network of 16 parallel channels (19 mm × 600 µm × 60–220 µm), in which the oxidative dehydrogenation of 3-methyl-2-buten-1-ol to aldehyde was carried out successfully for temperatures up to 464 °C [31]. The conversion increased smoothly with temperature and low oxygen and high alcohol concentrations were beneficial for selectivity, in addition to less deep channels (higher catalyst surface area to reaction channel volume). For temperatures ≥400 °C, the selectivity deteriorated due to CO and CO_2 formation.

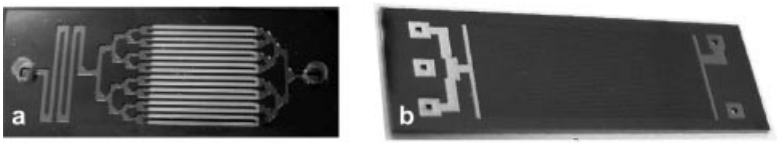

Figure 1.4 Microreactors with sputter-deposited catalysts: (a) chip (63 × 25 mm) with Ag film for oxidative dehydrogenation of 3-methyl-2-buten-1-ol to aldehyde (464 °C); (b) chip (3 × 1 cm) containing Pt, Fe or Co for (de)hydrogenation of cyclohexene (up to 250 °C) and synthesis gas methanation (up to 300 °C). Reprinted from [31], Copyright 2004, and [35], Copyright 2003, with permission from Elsevier.

Thin-films of 20 nm Fe, Co and Pt were DC magnetron sputter deposited in the channels of microreactors containing reaction manifolds of 39 or 780 parallel fluidic passages (dimensions: 19 mm × 100 μm × 100 μm and 18 mm × 5–10 μm × 5 μm, respectively) (Figure 1.4b), which were then exploited for investigations of synthesis gas methanation over Fe and Co (up to 300 °C) and the (de)hydrogenation of cyclohexene over Pt (up to 250 °C) [32–35]. Microreactors with Fe and Co catalysts were used for research on Fischer–Tropsch reaction mechanisms. Since cyclohexene is liquid under ambient conditions, C_6H_{10} vapor was fed to the microreactor by bubbling argon in the C_6H_{10} reservoir. The rate (or control)-limiting step for Pt-catalyzed (de)hydrogenation of C_6H_{10}, and hence the regime in which the microreactor operates, was identified as being reaction limited with the surface reaction as the rate-limiting step.

The applicability of microreactors with incorporated Pt-layers into serpentine-shaped reaction channels (14–42 cm × 0.5–1.5 mm × 100 μm) was evaluated by means of CO oxidation. This reaction was executed in channels containing a sputtered Pt film (20–200 nm) and channels filled with silicon pillars (diameter 20 μm) covered with a Pt/Al_2O_3 film via wash-coating and impregnation. Due to the increased active catalyst surface, the latter film showed the highest selectivity as a sensor for CO [36]. A micro flow-through membrane of porous silicon incorporated in a silicon-based microreactor can also be used as CO sensor (Figure 1.5). This device contains a permeable membrane of porous silicon (squares of 350–750 μm, thickness ∼70 μm) coated with palladium (via liquid immersion and drying). With integrated heaters and temperature elements, efficient CO measurements, based on resistivity changes of the porous membrane due to Pd-catalyzed CO conversion into CO_2, were performed for temperatures up to 140 °C [37]. When the permeable porous silicon is replaced by a thin (gas-tight) layer of stoichiometric silicon nitride (Si_3N_4) with gas-sensitive SnO_2 thin film, such a microreactor could be used for

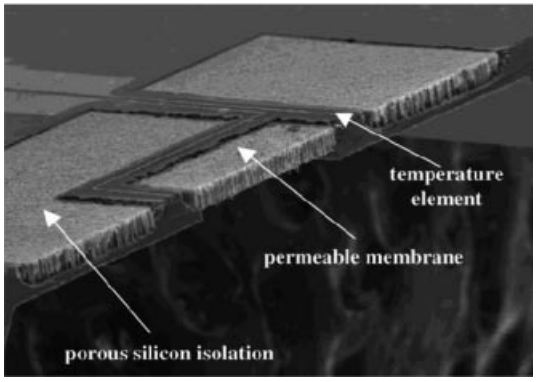

Figure 1.5 Microreactor with permeable porous silicon membrane (squares of 350–750 μm, thickness 70 μm) coated with Pd (via immersion) with heating filament and temperature sensor for CO measurements up to 140 °C. Reprinted from [37], Copyright 2002, with permission from Elsevier.

detection of pollution of air with CO, NO, NO_2 and/or O_3 for temperatures up to 400 °C [38].

Palladium thin films in microreactors can also be used for hydrogen purification, since hydrogen selectively permeates through a Pd layer via a process of dissociative chemisorption, reversible dissolution of atomic hydrogen, diffusion and desorption. Different microreactor designs for H_2 purification have been reported, all of which are based on revealing structural membrane support structures in silicon. For example, on the unetched side of an oxidized (110)-silicon wafer containing eight blocks of 125 individual deep grooves (1.5 mm × 23 μm wide on an area of 18 × 18 mm), a layer of 1 μm thick Pd–Ag film (77:23%) was co-sputtered. Openings to this pinhole-free separation membrane were made with KOH and BHF. Up to 450 °C, these membranes showed high permeation rates and selectivity for hydrogen (at least 1500 for H_2–He) [39]. Similar results were found for 200–500 nm thick Pd–Ag films deposited on the back side of a perforated SiO_2–SiN microsieve (circular holes of 5 μm diameter) that was supported by silicon with parallelogram-shaped openings (600 μm × 1.9–2.6 mm), resulting in a larger, less fragile area of Pd-Ag available for hydrogen permeation [40]. A more efficient way of heating Pd permeation membranes is the integration of thin-film structures on this membrane. With a microreactor (8 × 16 mm) containing Ta–Pt–Ta thin films (10:200:20 nm) on the top side of a perforated SiO_2–SiN microsieve (4 μm circular holes) and a sputtered Pd–Ag film on the back side, a nearly identical performance was achieved with significantly less electrical heating power to reach temperatures up to 350 °C [41], and also in a device (20 × 25 mm) comprising a square (5 × 5 mm) of 30 μm thick oxidized porous silicon, which served as a support (and thermal insulator) for a Pd membrane with an integrated Pt–Ti heater [42].

The endothermic catalytic steam reforming of methanol results in hydrogen, and microreactors with different catalysts have been fabricated for this reaction. In a reactor of UV-sensitive glass, a reaction zone containing 13 parallel channels (20 mm long, 500 μm wide, 1 mm deep) was realized and coated with a 30 μm thick Cu–ZnO layer (via a precipitation process). For temperatures up to ∼250 °C, reformate was produced with a hydrogen content up to 73% [43]. With this catalyst impregnated on particles that were loaded in a network of seven parallel, serpentine-shaped channels (1 mm × 200–400 μm) and fixed via a filter (retainer posts) in the exhaust manifold, reform reactions were carried out successfully up to 200 °C with methanol to hydrogen conversions up to 89%. Relatively low input powers were required due to integration of thin-film heaters and temperature sensors (20 nm Pt) on the back side of the oxidized silicon [44]. Very similar results, viz. hydrogen selectivities (at 200 °C) of 74 and 67% for Ni/SiO_2 and Co/SiO_2, respectively, were obtained with nanoscale-synthesized Co and Ni silica catalysts sol–gel coated in the reaction zone array (13 × 12 mm) consisting of parallel channels (50 × 100 μm) of a reactor (31 × 16 mm) [45].

In order to control highly exothermic catalytic partial oxidation reactions, small time constants for heating and cooling of gases are required. Microreactors equipped with a reaction channel that is capped on one side with a flat, thin, non-permeable membrane (∼1 μm thick) are very suitable for gas-phase reactions at temperatures

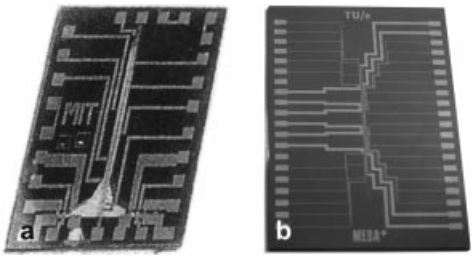

Figure 1.6 Flat-membrane microreactors: (a) chip (25 × 15 mm) for Pt-catalyzed ammonia oxidation (up to 600 °C); (b) chip (45 × 30 mm^2) for Rh-catalyzed oxidation of hydrogen and direct CPO of methane into syngas (>600 °C). (a) Reproduced from [46], (b) reprinted from [47], Copyright 2005, with permission from Elsevier.

up to 600 °C (Figure 1.6). On the outside of this membrane, metal thin-film heaters and temperature sensors were deposited for local heating and temperature sensing. Due to these integrated elements in combination with the composition of the membrane, gas heating-up and cooling-down times in the millisecond range were obtained, such that highly exothermic reactions could be controlled and carried out with improved selectivity and conversion [46, 47]. The thickness and material composition of flat membranes depends closely on thermal, mechanical, thermo-mechanical and electrical aspects. For example, membranes made of thermally and electrically insulating materials only (e.g. SiN) require extremely low input powers to reach high temperatures, but above ∼550 °C these membranes are unfavorable because of thermomechanical-induced stresses [46, 48]. Membranes that include a thin layer of (highly doped) silicon are (thermo)mechanically robust, but require more input energy to ignite a reaction, and thereby have larger heating-up time constants and can be subject to electrical breakdown problems above ∼700 °C [47]). Clearly, for each high-temperature reaction, a trade-off between these aspects is required to obtain the "optimal" flat membrane configuration, which can be found by detailed modeling [49–51]. Microreactors were realized with I-shaped and T-shaped reaction channels (20–30 mm × 0.5–1.3 mm × 500–550 μm) with sputtered Pt and Rh catalyst areas and equipped with thin-film control functionality of 100–200 nm Pt (adhesion layer 10 nm Ti or Ta). Localized hot reaction zones were used for studying the kinetics of Rh-catalyzed H_2 oxidation, Pt-catalyzed NH_3 oxidation and Rh-catalyzed direct oxidation of CH_4 into syngas, for reaction temperatures in the range 400–700 °C [46, 47].

Via inclusion of corrugations in the membrane which act as mechanical decoupling zones and compensate for thermally-induced mechanical stresses, microreactors were realized for operating temperatures above 700 °C, viz. silicon nitride-based tube structures of which the functionality is limited to ca. 900 °C due to degradation phenomena that occur in the integrated Pt-based thin-film heaters. A microreactor with silicon nitride tubes hanging freely in a flow channel (30 mm × 500 μm × 330 μm) was fabricated using a modified buried structure technology (Figure 1.7a). A Pt layer of

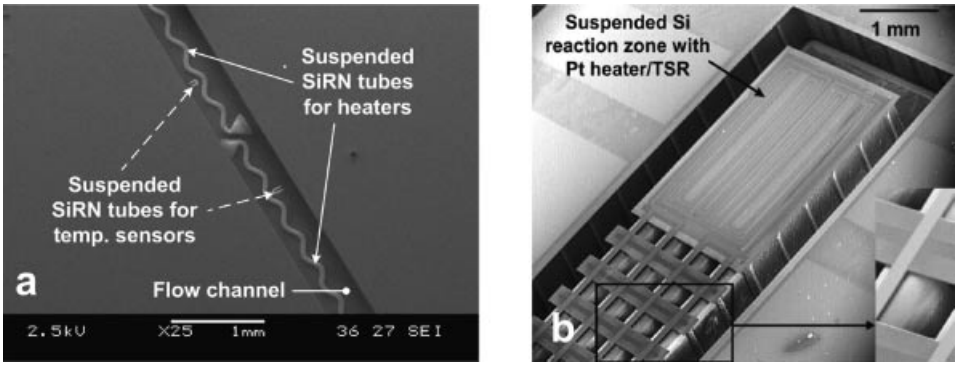

Figure 1.7 Microreactors with suspended tubes of silicon nitride: (a) tubes freely hanging in flow channel of chip (45 × 30 mm) for Rh-catalyzed direct partial oxidation of methane into synthesis gas (>600 °C); (b) U-shaped tubes for autothermal butane combustion (over Ir catalyst) and ammonia cracking (over Pt catalyst) for temperatures up to 900 °C. (a) From [52], reproduced by permission of The Royal Society of Chemistry; (b) reproduced from [53], with permission, Copyright 2003 IEEE.

200 nm in these tubes served as heaters and sensors [52]. Use of low-thermal conductivity silicon nitride as material also results in very efficient use of energy for performing reactions. A microreactor comprising two separate U-shaped suspended-tube fluid channels was developed for very efficient hydrogen production (Figure 1.7b). This suspended-tube reactor consisted of four thin-walled (∼2 μm) SiN-tubes (200 × 480 μm). On one end these tubes were fixed in a silicon substrate containing fluidic channels and ports, and on the other end the channels formed a free-standing structure. This free end (hot zone) was partially encased in silicon to form a thermally isolated region in which reactions could occur and these U-shapes could expand during operation to relieve stress. The tubes passed through isolated silicon slabs that permitted heat transfer between fluid streams in both U-shaped channels, without significantly adding heat loss. Heaters and sensors (200 nm Pt, 10 nm Ta) embedded on the tubes were used to initiate and control operation. In the microreactor/heat exchanger the catalytic autothermal (self-sustaining) butane combustion (wash-coated Ir) and ammonia cracking (wash-coated Pt) were achieved simultaneously for temperatures up to 900 °C, where the exothermic reaction in one stream provided the energy required for the endothermic reaction in the adjacent stream [53].

The examples discussed here represent only a small fraction of the many possible designs, applications and versatility of silicon- and glass-based microreactor platforms. Currently these devices are in particular applied for research purposes and to a lesser extent for small-scale on-demand production of pure fine chemicals, portable fuel cell and other power source applications. To obtain larger production of compounds, the concept of scale-up/scale-out by replication of many stacked or parallel arranged units, resulting in microfabrication plants, is proposed, although this approach induces complex challenges in integration of fluid handling, local reactor monitoring and control [54, 55].

1.3
Design and Fabrication of Microreactors for High-pressure Applications

Recently, the fabrication of microreactors for high-pressure applications was reported, since it is well known that pressure has a positive influence on many chemical processes. For example, for reactions that have a negative molar activation or molar reaction volume, rate enhancements and shifts in equilibrium position occur at higher pressures. In this case, pressure increase becomes effective above a few kilobar. A beneficial effect that occurs at much lower pressures (up to ca. 100 bar) is the suppression of the boiling point of organic solvents, by which it becomes possible to perform liquid-phase reactions at higher temperatures and thus with higher reaction rates. An example of this is a microreactor which is capable of reaching pressures exceeding 100 bar, under which conditions it is possible to operate above the boiling point of toluene in Heck aminocarbonylation reactions [56]. A recently developed solder-based sealing technique was used for the fluidic connections [57]. Finally, reactions in liquid solvents that involve gases such as hydrogen or oxygen benefit from a higher pressure (up to several tens of bar) because the solubility of the gases increases.

Microreactors are beneficial for performing reactions at high pressures, because of the reduced risks of damage after failure of the reactor: the energy, being the product of pressure and volume, released in, for example, an explosion can be kept low due to the small volume. Working pressures of at least 700 bar can be realized in a microreactor, but are limited by the fluidic connections [58]. Glass microreactors with in-plane interface geometries with glued capillaries were used to study pressure sensitive Diels-Alder reactions and phase-change dynamics in CO_2-alcohol mixtures (via optical microscopy) for temperatures and pressures in the ranges 35–95 °C and 60–150 bar (Figure 1.8). A fluidic resistor after the reaction channel ensured high pressure in this heated zone. Significant rate enhancements were found for fairly low pressure conditions [59]. Silicon-glass microreactors were utilized for studying multiphase microfluidics at elevated pressures, resulting in gas–liquid flows near the sonic velocity limit with a remaining laminar gas phase (provided that the flow

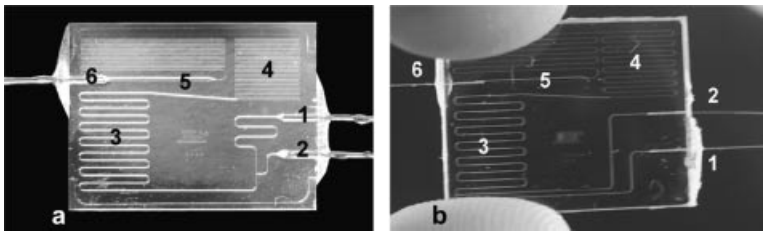

Figure 1.8 Glass microreactors with in-plane interface geometries with glued capillaries with a diameter of (a) 360 or (b) 110 µm for reaction conditions in the window 35–95 °C, 60–150 bar. **1**, **2**, Inlets for pressurized fluids; **3**, reaction zone; **4**, fluidic resistor; **5**, expansion zone; **6**, outlet. Reprinted from [58], Copyright 2007, with permission from Elsevier.

channel was narrower than 100 μm) [60], and also for performing the Pd-catalyzed hydrogenation of cyclohexene for pressures up to 140 bar (temperature 80 °C) [61]. Increased reaction rates were found for a packed bed containing Pd coated on carbon particles.

Interesting other applications of high-pressure microreactors are related to the use of "green" alternatives for organic solvents such as supercritical (*sc*) CO_2 and H_2O, of which the supercritical points (31.1 °C/73.9 bar and 374 °C/220 bar, respectively) are accessible in microreactors. For example, in a glass microreactor with a serpentine-shaped channel (length 40 cm, cross-sectional radius 100 μm), Pd-catalyzed hydrogenation reactions were performed with *sc*CO_2 as a solvent. Palladium was immobilized on the glass walls and high conversions were found for residence times of one second [62]. Although supercritical fluids are attractive media for synthetic chemistry (higher selectivity and reaction rates, better yields), the use of *sc*H_2O in silicon–glass reactors might be a problem due to its corrosive nature. Another issue that has to be taken into account is that the intrinsic microreactor safety might no longer hold at sufficiently high pressures, due to the dependence of homogeneous reactions on pressure: above a certain pressure: channel diameter ratio, suppression of homogeneous reactions (e.g. flames, explosions) and kinetic quenching of radical chain mechanisms can no longer be achieved [63].

1.4
Microreactors for Liquid-phase Organic Chemistry and Biochemistry

1.4.1
Integrated Microfluidic Networks for High-throughput Experiments

In the previous sections, we have discussed the use of microreactors for performing reactions that either generate large amounts of heat, require extreme conditions such as high pressures or high temperatures or require a high surface-to-volume ratio to enhance conversion on a solid catalyst (generally also a medium- to high-temperature process). Although *heat transport* can be a major concern in gas-phase reactions, in most liquid-phase reactions *mass transport* is the limiting factor. This simply follows from the respective molecular diffusion constants, which are four or more orders of magnitude higher in the gas phase than in the liquid phase, and the respective thermal conductivities, which are typically one order of magnitude higher in a liquid (compared with gas at 1 atm). Therefore, achieving adequate mixing of reactants is an important challenge in the liquid phase. Since this topic has been discussed extensively in another chapter, we will not discuss it here, although many different static mixer designs have been implemented in silicon and glass microreactors. The important point about the use of micromachining techniques is that static mixer concepts are easily integrated with complex microfluidic reaction networks because the photolithographic and etching processes are performed on a wafer scale in a monolithic fashion.

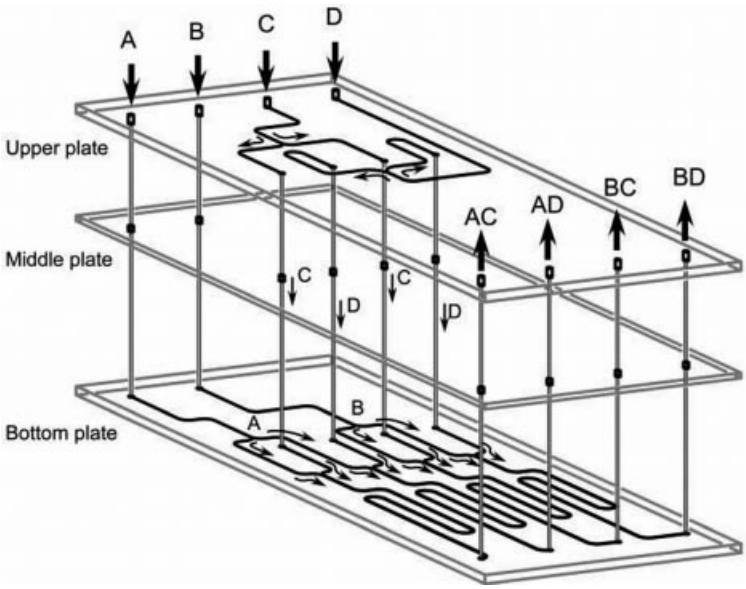

Figure 1.9 Schematic view of three-dimensional microchannel circuit inside the microchip for combinatorial chemistry. Reproduced from [66], with permission.

Similarly, many reactors with integrated mixers and other functionality can be manufactured on one substrate to form, e.g., a combinatorial synthesis platform. Such microfluidic platforms may approach the complexity of VLSI electronic circuits, see e.g. [64], which gives an example fabricated by "soft lithography" (imprinting) in the polymer PDMS or [65], which gives an example in laser-machined laminated Mylar sheets. The combinatorial aspect of these examples consists in mixing chemicals in different ratios to achieve concentration series in a discrete way (i.e. a different concentration for each microchannel) which are subsequently used in a chemical reaction on the same microfluidic chip.

An example of this concept has been given for a glass chip, as shown in Figure 1.9 [66]. A specialty of the latter chip is that it involves a phase-transfer process between two parallel streams, one of an aqueous and the other of an immiscible organic phase. The amine in the aqueous phase diffuses into the organic phase and reacts with acid chloride, an amide, which remains in the organic phase, and an inorganic salt, which diffuses back into the aqueous phase, are formed as products. It may be evident that such phase-transfer processes benefit from a large interfacial area and short diffusion distances, which implies that microreactor technology helps in performing such reactions efficiently. Another demonstration of the use of a so-called "phase-transfer catalyst" in a glass microchannel reactor was given by Ueno *et al.* for the benzylation of ethyl-2-oxocyclopentane carboxylate with benzyl bromide in Taylor flow with segments of CH_2Cl_2 and NaOH [67].

Instead of concentration gradients, the use of temperature gradients is also an interesting concept for use in high-throughput reaction kinetics studies. An example

of this is the work of Mao *et al.* [68], who established a linear temperature gradient from 10 to 80 °C over 36 parallel microchannels, by connecting the channel network to a hot fluid flowing on one side of the array of channels (close to channel 1) and a cold fluid flowing on the other side (close to channel 36). The device was based on a combination of brass and PDMS parts and was used to study temperature-dependent fluorescence of nanoparticles, activation energies of catalytic reactions and melting point transitions of lipid membranes.

An example of a temperature gradient created on a silicon microfluidic chip with integrated heater patterns is the work on polymerase chain reaction (PCR) by Kopp *et al.* [69]. The idea behind their chip design is that the DNA sample to be amplified flows through three subsequent temperature zones, of 95 °C for melting of the DNA, 60 °C for annealing and 77 °C for extension of the DNA. After this, the sample flows through the 95 °C zone again, etc. Hence, instead of cycling the temperature *in time* in a batch reactor, the temperature cycling is performed *in space* in a flow reactor. The residence time at each temperature is controlled by the length of the microchannel in the particular temperature zone.

Analogously, it is possible to perform a reaction at *different residence times* simultaneously, by creating parallel channels of different length and applying the same flow rate through each microchannel. This concept was tested with success for a homogeneously catalyzed Knoevenagel condensation by Bula *et al.* for up to four parallel channels, i.e. four different reaction periods simultaneously [70], but with the micromachining technology available the concept can easily be extended to a much higher number of reaction periods. An important lesson of this work is that, although a large number of reactions can be carried out in parallel with very limited amounts of material (several hundred nanoliters) and in a short time span, the real merits of the parallel concept can only be appreciated if an integrated analysis method can be used to evaluate the conversion of reactants on-line (or in-line). Bula *et al.* [70] performed product analysis off-line using UV absorption, by quenching the reaction mixture in-line and collecting the resulting liquid. Therefore, although the reaction times studied were only a few minutes, in order to have enough sample for analysis with state-of-the-art spectroscopic equipment, product had to be collected for several hours. The as yet limited availability of integrated analysis methods, examples being the integrated waveguides reported by Kraus *et al.* [71] and Mogensen *et al.* [72] and the integrated NMR microcoils studied by Wensink *et al.* [73], is a general problem in the microreactor field, more details about this topic can be found in Volume 3 of this Handbook.

1.4.2
Microreactors Employing Immobilized Molecular Catalysts

Because of the simplicity, in synthetic organic chemistry use is frequently made of homogeneous (molecular) catalysts to enhance selectivity and reaction rate. Examples are transition metal ions and complexes, (in)organic acids and bases and enzymes. Although this has the advantage of a high effective concentration of the catalyst, compared with a heterogeneous catalyst, thereby allowing the same reaction

rate under milder conditions with greater selectivity, a serious drawback is that the catalyst has to be separated after reaction.

For a large range of chemistries, this problem may be solved by immobilizing the catalyst on the surface of a bead of polystyrene, PEG or polyacrylamide resin or of silica or another type of glass. The beads can be separated after reaction by simple filtration or, more sophistically, using magnetic fields in case the beads contain a magnetic material.

This bead-based procedure is a derivative of the "solid-phase chemistry" that has proven its merits in automated peptide synthesis [74], combinatorial chemistry [75] and also small-molecule synthesis [76]. The basic principle behind solid-phase synthesis is the attachment of a *substrate* to a polymer bead by a covalent linker and subsequently performing a chemical reaction on the substrate. Because the substrate is tightly bound to the polymer, excess reagents and by-products can simply be washed away, after which further chemical elaboration of the product may be performed. Finally, the clean product is cleaved from the polymeric support, which usually can be regenerated for re-use.

Although solid-phase chemistry traditionally has been performed in batch reactors, it can easily be implemented in a continuous-flow fashion (see [77] for a review), in analogy to the packed beds used in chromatography. Similarly to the current trend in HPLC, monolithic supports may replace the beads [77].

Employing glass frits to block the beads, solid-phase chemistry, as mentioned above, has been carried out in a glass microreactor. Beads of Amberlyst-15, which is a sulfonic acid-based cation-exchange resin, were employed for the acid-catalyzed deacetalization of 11 dimethylacetals to their respective aldehydes with high yield (over 95%) and excellent purity (better than 99%) without the need for further product purification [78]. Several other examples exist of similar experiments with catalysts or reactants immobilized on beads which were packed in glass or polymer microreactors, with principally the same results. However, although there is no fundamental reason why the same immobilization chemistry that is used for substrates and molecular catalysts on beads and monoliths should not be applicable directly to the inner walls of a glass or oxidized silicon (or polymer-coated) microreactor, it seems that this has hardly been investigated. The latter certainly is a route for further research.

One typical result with respect to the latter is worth mentioning here. Brivio *et al.* [79] found that the surface of glass chips themselves may act as an acid catalyst in synthetic organic chemistry. This is related to the silanol groups that are present on the glass surface. Care should thus be taken in cases where such acidic effects are unwanted, e.g. by passivating the glass surface with specific coatings. An example has been reported [80] for the case of a glass PCR microchip.

1.4.3 Enzymatic Microreactors

One category of microreactors in which immobilized (molecular) catalysts are extensively used is that of the *enzyme microreactors*. Although it is possible to perform

enzymatic reactions with enzymes in solution, for reasons of recycling of the enzyme and to avoid the enzymes being adsorbed in the microreactor in unwanted locations or in a non-specific way, it is desirable to immobilize the enzymes. This immobilization should, however, be very specific; non-specific adsorption may lead to deactivation or even denaturation of the enzymes. The reasons for using enzymes are obvious: many of the substances that we want to synthesize are only obtainable in high purity in the right enantiomeric conformation and in a limited number of subsequent chemical reactions by the use of specific enzymes.

Literature on enzyme microreactors *for chemical synthesis* is scarce. There is abundant literature, however, on the use of enzymes in microsystems for purposes of DNA analysis, e.g. using the polymerase chain reaction discussed before or DNA restriction fragment analysis [81], for proteomics, such as tryptic digestion of proteins with the enzyme free in solution [82], with trypsin-coated beads trapped in a microreactor [83] or trypsin immobilized on a porous polymer monolith (in a fused-silica capillary) [84]. Also, enzyme microreaction devices have been used extensively for medical diagnostics or immunoassays, e.g. using porous silicon as a support for immobilized enzymes [85].

In the field of organic synthesis, it was reported that the catalytic hydrolysis of umbelliferone esters (7-acetoxycoumarin) to 7-hydroxycoumarin by porcine pancreatic lipase covalently immobilized on microchannel reactors almost completed within 1 min, to be compared with 4 min in a normal batch reaction [86]. The same group demonstrated an improvement in the yield of trypsin-catalyzed hydrolysis of benzoylarginine-*p*-nitroanilide in a microchannel reactor with a lower enzyme concentration but a 20-fold higher reaction rate than in a batch reactor [87].

Other examples are enzymes immobilized on beads which are trapped in a microreactor by etched weirs [88], enzymes encapsulated in hydrogel patches or sol–gel silica [89] and enzymes attached on the surface of (porous) microstructures (for example, on porous silicon manufactured by anodization of single-crystalline silicon; see Figure 1.10 [91]), of mesoporous silica or polymer monoliths or directly

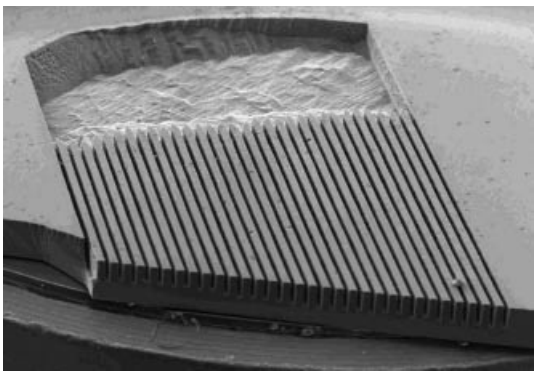

Figure 1.10 Silicon enzyme microreactor containing parallel channels with a porous silicon layer. Reprinted from [91], Copyright 2002, with permission from Elsevier.

or indirectly to microchannel walls (e.g. via covalent binding or avidin–biotin binding [91].

1.4.4 Synthesis of Bio-related Compounds: Peptides and Sugars

The formation of large sugar molecules, oligosaccharides, in a process called glycosylation, is often a difficult process that requires extensive optimization regarding the type of anomeric leaving group, solvent, reaction temperature and reaction time. Experimental effort and valuable starting materials can be reduced considerably by using a microreactor-based approach in combination with a chromatographic technique. Because of the sensitivity to moisture and the use of aggressive solvents in the glycosylation process, silicon is an attractive choice of material, which, because of its high thermal conductivity, also allows rapid thermal equilibration and temperature control. The microreactor shown in Figure 1.11 has three inlets, for the glycosylating agent, the activator and the nucleophile, a simple serpentine channel mixer and a longer reaction coil, which close to the outlet has an inlet for a quenching agent [92, 93]. With this reactor, in 1 day 40 experimental conditions could be tested, whereas with conventional glassware, in the same period only three conditions could be tested.

Watts *et al*. demonstrated multi-step solution-phase synthesis of peptides in a glass microreactor with quantitative yield in 20 min [94]. This should be compared with batch reactions where only moderate yields (40–50%) were obtained in 24 h. Common protecting groups were used, viz. Fmoc was selected for N-protection and Dmab ester for protection of the carboxylic acid. The reaction was carried out in the microreactor under electroosmotic flow. Deprotection, which is required to extend the peptide chains beyond dipeptides, was also demonstrated with quantitative yield in the microreactor. In this first microreactor demonstration, only alanine-based peptides were synthesized; in later work other amino acids were also used [95, 96].

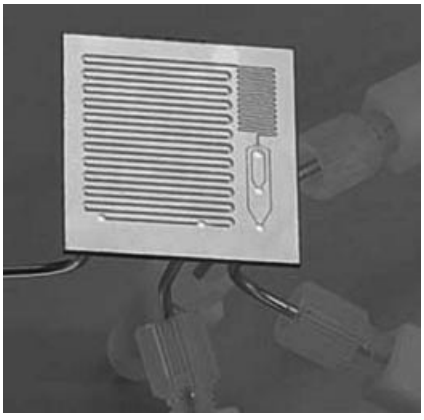

Figure 1.11 Silicon microfluidic microreactor for glycosylation. Reproduced from [92], with permission.

Flögel *et al*. [97] described a silicon microreactor (the same as in Figure 1.11) for peptide synthesis, which also allows a quick screening of reaction conditions. Using peptide couplings with Boc- and Fmoc-protected amino acids, significant amounts of peptides could be made in 1–5 min at temperatures as high as 120 °C. Synthesis efficiency was further enhanced by the use of a fluorous benzyl tag for the assembly of β-peptides; this method is particularly useful for the purification of poorly soluble products.

1.5 Conclusion

In this chapter, the use of silicon and glass as a material for microreactors has been discussed. The use of these materials has the major advantage that a large number of techniques, derived from microelectronics and MEMS, exist, which allow the fabrication of complex and integrated microfluidic networks in parallel. These microreactors can be applied to almost all the chemistry that is normally done in glassware, but with all the advantages of microreaction technology. Many applications of this reactor type have been discussed, including high-temperature and high-pressure experiments, high-throughput screening applications, homogeneous and heterogeneous catalytic processes and processes employing immobilized enzymes.

Although not discussed in detail in this chapter, in addition to the use in a research laboratory environment, microfluidic systems in glass and silicon may be used for chemical production, if economic ways of scaling-out can be realized. As demonstrated by the very successful microprocessor and computer industry, which is based on the same processes as described in this chapter, the technology to do this is available.

References

1 W. Ehrfeld, V. Hessel, H. Löwe, *Microreactors: New Technology of Modern Chemistry*, Wiley-VCH Verlag GmbH, Weinheim, **2000**.

2 V. Hessel, S. Hardt, H. Löwe, *Chemical Micro Process Engineering: Fundamentals, Modelling and Reactions*, Wiley-VCH Verlag GmbH, Weinheim, **2004**.

3 K. Jähnisch, V. Hessel, H. Löwe, M. Baerns, *Angew. Chem. Int. Ed.* **2004**, *43*, 406–446.

4 M. Elwenspoek, H. V. Jansen, *Silicon Micromachining*, Cambridge University Press, Cambridge, **1998**.

5 M. J. Madou, *Fundamentals of Microfabrication: the Science of Miniaturization*, 2nd edn, CRC Press, Boca Raton, FL, **2002**.

6 J. G. E. Gardeniers, A. van den Berg, Microfabrication and integration in *Separation Methods in Microanalytical Systems* (eds J. P. Kutter, Y. Fintschenko), CRC Press, Boca Raton, FL, **2006**, 55–106.

7 K. E. Petersen, *Proc. IEEE*, **1982**, *70*, 420–457.

8 J. G. E. Gardeniers, R. E. Oosterbroek, A. van den Berg, Silicon and glass micromachining for μTAS, in *Lab-on-a-Chip, Miniaturized Systems for (Bio)chemical Analysis and Synthesis* (eds Oosterbroek, A. van den Berg), Elsevier, Amsterdam, **2003**, 37–64.

9 R. Knitter, T. R. Dietrich, Microfabrication in ceramics and glass, in *Advanced Micro and Nanosystems, Vol. 5: Micro Process Engineering – Fundamentals, Devices, Fabrication and Applications* (eds O. Brand, G. K. Fedder, C. Hierold, J. G. Korvink, O. Tabata, N. Kockmann), Wiley-VCH Verlag GmbH, Weinheim, **2006**, 353–385.

10 Y. S. S. Wan, J. L. H. Chau, A. Gavriilidis, K. L. Yeung, *Micro Mesopor. Mater.* **2001**, *42*, 157–175.

11 J. L. H. Chau, Y. S. S. Wan, A. Gavriilidis, K. L. Yeung, *Chem. Eng. J.* **2002**, *88*, 187–200.

12 J. L. H. Chau, K. L. Yeung, *Chem. Commun.* **2002**, 960–961.

13 L. Kiwi-Minsker, A. Renken, *Catal. Today* **2005**, *110*, 2–14.

14 Y. S. S. Wan, A. Gavriilidis, K. L. Yeung, *Trans. Inst. Chem Eng.* **2003**, *81*, 753–759.

15 Y. S. S. Wan, J. L. H. Chau, K. L. Yeung, A. Gavriilidis, *J. Catal.* **2004**, *223*, 241–249.

16 J. Kobayashi, Y. Mori, K. Okamoto, R. Akiyama, M. Ueno, T. Kitamori, S. Kobayashi, *Science* **2004**, *304*, 1305–1308.

17 S. K. Ajmera, M. W. Losey, K. F. Jensen, M. A. Schmidt, *AIChE J.* **2001**, *47*, 1639–1647.

18 M. W. Losey, M. A. Schmidt, K. F. Jensen, *Ind. Eng. Chem. Res.* **2001**, *40*, 2555–2562.

19 M. W. Losey, R. J. Jackman, S. L. Firebaugh, M. A. Schmidt, K. F. Jensen, *J. Microelectromech. Syst.* **2002**, *11*, 709–717.

20 S. K. Ajmera, C. Delattre, M. A. Schmidt, K. F. Jensen, *J. Catal.* **2002**, *209*, 401–412.

21 S. K. Ajmera, C. Delattre, M. A. Schmidt, K. F. Jensen, *Sens. Actuators B* **2002**, *82*, 297–306.

22 K. Kusakabe, K. Tokunaga, G. Zhao, K. Sotowa, S. Morooka, *J. Chem. Eng. Jpn.* **2002**, *35*, 914–917.

23 H. Chen, L. Bednarova, R. S. Besser, W. Y. Lee, *Appl. Catal. A* **2005**, *286*, 186–195.

24 S. Srinivas, A. Dhingra, H. Im, E. Gulari, *Appl. Catal. A* **2004**, *274*, 285–293.

25 X. Ouyang, L. Bednarova, R. S. Besser, P. Ho, *AIChE J.* **2005**, *51*, 1758–1772.

26 S. Thybo, S. Jensen, S. Johansen, T. Johannessen, O. Hansen, U. Quaade, *J. Catal.* **2004**, *223*, 271–277.

27 O. Younes-Metzler, J. Svagin, S. Jensen, C. H. Christensen, O. Hansen, U. Quaade, *Appl. Catal. A* **2005**, *284*, 5–10.

28 O. Younes-Metzler, J. Johansen, S. Thorsteinsson, S. Jensen, O. Hansen, U. J. Quaade, *J. Catal.* **2006**, *241*, 74–82.

29 A. Klerke, S. Saadi, M. B. Toftegaard, A. T. Madsen, J. H. Nielsen, S. Jensen, O. Hansen, C. H. Christensen, U. J. Quaade, *Catal. Lett.* **2006**, *109*, 7–12.

30 R. Z. Sørensen, A. Klerke, U. Quaade, S. Jensen, O. Hansen, C. J. Christensen, *Catal. Lett.* **2006**, *112*, 77–81.

31 E. Cao, A. Gavriilidis, W. B. Motherwell, *Chem. Eng. Sci.* **2004**, *59*, 4803–4808.

32 R. S. Besser, X. Ouyang, H. Surangalikar, *Chem. Eng. Sci.* **2003**, *58*, 19–26.

33 R. S. Besser, *Chem. Eng. Commun.* **2003**, *190*, 1293–1308.

34 H. Surangalikar, X. Ouyang, R. S. Besser, *Chem. Eng. J.* **2003**, *93*, 217–224.

35 X. Ouyang, R. S. Besser, *Catal. Today* **2003**, *84*, 33–41.

36 M. Roumanie, C. Pijolat, V. Meille, C. De Bellefon, P. Pouteau, C. Delattre, *Sens. Actuators B* **2006**, *118*, 297–304.

37 A. Splinter, J. Stürmann, O. Bartels, W. Benecke, *Sens. Actuators B* **2002**, *83*, 169–174.

38 T. Becker, S. Mühlberger, C. Bosch-v. Braunmühl, G. Müller, A. Meckes, W. Benecke, *J. Microelectromech. Syst.* **2000**, *9*, 478–484.

39 H. D. Tong, J. W. Berenschot, M. J. de Boer, J. G. E. Gardeniers, H. Wensink, H. V. Jansen, W. Nijdam, M. C. Elwenspoek, F. C. Gielens, C. J. M. van Rijn, *J. Microelectromech. Syst.* **2003**, *12*, 622–629.

40 H. D. Tong, F. C. Gielens, J. G. E. Gardeniers, H. V. Jansen, J. W. Berenschot, M. J. de Boer, J. H. de Boer, C. J. M. van Rijn, M. C. Elwenspoek, *J. Microelectromech. Syst.* **2005**, *14*, 113–124.

41 B. A. Wilhite, M. A. Schmidt, K. F. Jensen, *Ind. Eng. Chem. Res.* **2004**, *43*, 7083–7091.

42 S. Y. Ye, S. Tanaka, M. Esashi, S. Hamakawa, T. Hanaoka, F. Mizukami, *J. Micromech. Microeng.* **2005**, *15*, 2011–2018.

43 T. Kim, S. Kwon, *J. Micromech. Microeng.* **2006**, *16*, 1760–1768.

44 A. V. Pattekar, M. V. Kothare, *J. Microelectromech. Syst.* **2004**, *13*, 7–18.

45 K. Shetty, S. Zhao, W. Cao, U. Siriwardane, N. V. Seetala, D. Kuila, *J. Power Sources* **2007**, *163*, 630–636.

46 R. Srinivasan, I.-M. Hsing, P. E. Berger, S. L. Firebaugh, M. A. Schmidt, M. P. Harold, J. J. Lerou, J. F. Ryley, *AIChE J.* **1997**, *43*, 3059–3069.

47 R. M. Tiggelaar, P. van Male, J. W. Berenschot, J. G. E. Gardeniers, R. E. Oosterbroek, M. H. J. M. de Croon, J. C. Schouten, A. van den Berg, M. C. Elwenspoek, *Sens. Actuators A* **2005**, *119*, 196–205.

48 C. Alépée, L. Vulpescu, P. Cousseau, P. Renaud, R. Maurer, A. Renken, *Meas. Control* **2000**, *33*, 65–268.

49 I.-M. Hsing, R. Srinivasan, M. P. Harold, K. F. Jensen, M. A. Schmidt, *Chem. Eng. Sci.* **2000**, *55*, 3–13.

50 D. J. Quiram, I.-M. Hsing, A. J. Franz, K. F. Jensen, M. A. Schmidt, *Chem. Eng. Sci.* **2000**, *55*, 3065–3075.

51 R. M. Tiggelaar, P. W. H. Loeters, P. van Male, R. E. Oosterbroek, J. G. E. Gardeniers, M. H. J. M. de Croon, J. C. Schouten, M. C. Elwenspoek, A. van den Berg, *Sens. Actuators A* **2004**, *112*, 267–277.

52 R. M. Tiggelaar, J. W. Berenschot, J. H. de Boer, R. G. P. Sanders, J. G. E. Gardeniers, R. E. Oosterbroek, A. van den Berg, M. C. Elwenspoek, *Lab Chip* **2005**, *5*, 326–336.

53 L. R. Arana, S. B. Schaevitz, A. J. Franz, M. A. Schmidt, K. F. Jensen, *J. Microelectromech. Syst.* **2003**, *12*, 600–612.

54 K. F. Jensen, *Chem. Eng. Sci.* **2001**, *56*, 293–303.

55 K. F. Jensen, *MRS Bull.* **2006**, *31*, 101–107.

56 E. R. Murphy, J. R. Martinelli, N. Zaborenko, S. L. Buchwald, K. F. Jensen, *Angew. Chem. Int. Ed.* **2007**, *46*, 1734–1737.

57 E. R. Murphy, T. Inoue, H. R. Sahoo, N. Zaborenko, K. F. Jensen, *Lab Chip* **2007**, *7*, 1309–1314.

58 R. M. Tiggelaar, F. Benito-López, D. C. Hermes, H. Rathgen, R. J. M. Egberink, F. G. Mugele, D. N. Reinhoudt, A. van den Berg, W. Verboom, J. G. E. Gardeniers, *Chem. Eng. J.* **2007**, *131*, 163–170.

59 F. Benito López, R. M. Tiggelaar, K. Salbut, J. Huskens, R. J. M. Egberink, D. N. Reinhoudt, H. J. G. E. Gardeniers, W. Verboom, *Lab Chip* **2007**, *7*, 1345–1351.

60 A. Günther, K. F. Jensen, in *Proceedings of the 10th International Conference on Miniaturized Systems for Chemistry and Life Sciences (μTAS 2006)*, 5–9 November 2006 Tokyo, **2006**, pp. 537–539.

61 F. Trachsel, C. Hutter, P. R. von Rohr, in *Proceedings of the 9th International Conference on Microreaction Technology (IMRET9)*, 6–8 September 2006, Potsdam, **2006**, pp. 349–350.

62 J. Kobayashi, Y. Mori, S. Kobayashi, *Chem. Commun.* **2005**, 2567–2568.

63 S. Chattopadhyay, G. Veser, *AIChE J.* **2006**, *52*, 2217–2229.

64 T. Thorsen, S. J. Maerkl, S. R. Quake, *Science* **2002**, *298*, 580–584.

65 C. Neils, Z. Tyree, B. Finlayson, A. Folch, *Lab Chip* **2004**, *4*, 342–350.

66 Y. Kikutani, T. Horiuchi, K. Uchiyama, H. Hisamoto, M. Tokeshia, T. Kitamori, *Lab Chip* **2002**, *2*, 188–192.

67 M. Ueno, H. Hisamoto, T. Kitamori, S. Kobayashi, *Chem. Commun.* **2003**, 936–937.

68 H. Mao, T. Yang, P. S. Cremer, *J. Am. Chem. Soc.* **2002**, *124*, 4432–4435.

69 M. U. Kopp, A. de Mello, A. Manz, *Science* **1998**, *280*, 1046–1048.

70 W. P. Bula, K. Kristianto, J. G. E. Gardeniers, W. Verboom, A. van den Berg, D. N. Reinhoudt, in *Proceedings of the 9th International Conference on Microreaction Technology (IMRET9)*, 6–8 September 2006, Potsdam, **2006**, 134–135.

71 T. Kraus, A. Günther, N. De Mas, M. A. Schmidt, K. F. Jensen, *Exp. Fluids* **2004**, *36*, 819–839.

72 K. B. Mogensen, N. J. Petersen, J. Hübner, J. P. Kutter, *Electrophoresis* **2001**, *22*, 3930–3938.

73 H. Wensink, F. Benito-Lopez, D. C. Hermes, W. Verboom, J. G. E. Gardeniers, D. N. Reinhoudt, A. van den Berg, *Lab Chip* **2005**, *5*, 280–284.

74 R. R. Merrifield, *J. Am. Chem. Soc.* **1963**, *85*, 2149–2154.

75 K. S. Lam, M. Lebl, V. Krchňák, *Chem. Rev.* **1997**, *97*, 411–448.

76 B. A. Bunin, J. A. Ellman, *J. Am. Chem. Soc.* **1992**, *114*, 10997–10998.

77 G. Jas, A. Kirschning, *Chem. Eur. J.* **2003**, *9*, 5708–5723.

78 C. Wiles, P. Watts, S. J. Haswell, *Tetrahedron* **2005**, *61*, 5209–5217.

79 M. Brivio, R. E. Oosterbroek, W. Verboom, M. H. Goedbloed, A. van den Berg, D. N. Reinhoudt, *Chem. Commun.* **2003**, 1924–1925.

80 B. C. Giordano, E. R. Copeland, J. P. Landers, *Electrophoresis* **2001**, *22*, 334–340.

81 S. C. Jacobson, J. M. Ramsey, *Anal. Chem.* **1996**, *68*, 720–723.

82 N. Gottschlich, C. T. Culbertson, T. E. McKnight, S. C. Jacobson, J. M. Ramsey, *J. Chromatogr. B* **2000**, *745*, 243–249.

83 C. Wang, R. Oleschuk, F. Ouchen, J. Li, P. Thibault, D. J. Harrison, *Rapid Commun. Mass Spectrom.* **2000**, *14*, 1377–1383.

84 D. S. Peterson, T. Rohr, F. Svec, J. M. J. Fréchet, *Anal. Chem.* **2002**, *74*, 4081–4088.

85 J. Yakovleva, R. Davidsson, A. Lobanova, M. Bengtsson, S. Eremin, T. Laurell, J. Emnéus, *Anal. Chem.* **2002**, *74*, 2994–3004.

86 M. Miyazaki, H. Maeda, *Trends Biotechnol.* **2006**, *24*, 463–470.

87 M. Miyazaki, H. Nakamura, H. Maeda, *Chem. Lett.* **2001**, 442–443.

88 R. D. Oleschuk, L. L. Shultz-Lockyear, Y. B. Ning, D. J. Harrison, *Anal. Chem.* **2000**, *72*, 585–590.

89 H. Y. Qu, H. T. Wantg, Y. Huang, W. Zhong, H. J. Lu, J. L. Kong, P. Y. Yang, B. H. Liu, *Anal. Chem.* **2004**, *76*, 6426–6433.

90 L. N. Amankwa, W. G. Kuhr, *Anal. Chem.* **1992**, *64*, 1610–1613.

91 M. Bengtson, S. Ekström, G. Marko-Varga, T. Laurell, *Talanta* **2002**, *56*, 341–353.

92 D. M. Ratner, E. R. Murphy, M. Jhunjhunwala, D. A. Snyder, K. F. Jensen, P. H. Seeberger, *Chem. Commun.* **2005**, 578–580.

93 K. Geyer, P. H. Seeberger, *Helv. Chim. Acta* **2007**, *90*, 395–403.

94 P. Watts, C. Wiles, S. J. Haswell, E. Pombo-Villar, P. Styring, *Chem. Commun.* **2001**, 990–991.

95 P. Watts, C. Wiles, S. J. Haswell, E. Pombo-Villar, *Tetrahedron* **2002**, *58*, 5427–5439.

96 P. Watts, C. Wiles, S. J. Haswell, E. Pombo-Villar, *Lab Chip* **2002**, *2*, 141–144.

97 O. Flögel, J. D. C. Codée, D. Seebach, P. H. Seeberger, *Angew. Chem. Int. Ed.* **2006**, *45*, 7000–7003.